Synthesis and Characterization of Nickel(II) and Palladium(II) Pyrrolyl Complexes and Their Polymerization to Electroactive Materials

Matthew Mathis, Wayne Harsha, and T. W. Hanks*

Department of Chemistry, Furman University, Greenville, South Carolina 29613

Rosa D. Bailey, George L. Schimek, and William T. Pennington

Department of Chemistry, Hunter Chemistry Laboratories, Clemson University, Clemson, South Carolina 29631

Received May 7, 1998. Revised Manuscript Received August 14, 1998

Four new transition metal−pyrrolyl complexes, bis(pyridyl)bis(pyrrolyl)palladium(II), (2,2′-bipyridyl)bis(pyrrolyl)palladium(II), (6-phenyl-2,2′-bipyridine)(pyrrolyl)palladium(II), and bis-(trimethylphosphino)(pyrrolyl)nickel(II) chloride, have been prepared and characterized. DFT calculations indicate that radical cations of the palladium compounds and their dimers have spin densities primarily on the pyrrolyl ligand, while the spin density of the nickel species radical is diffuse. Each complex was found to undergo oxidative polymerization to semiconducting polymers with good thermal properties. Polymers prepared with dodecylbenzenesulfonate as the counterion were soluble and could be cast into smooth, films with good physical properties.

Introduction

Functional polymers containing both highly conjugated backbones and high loadings of transition metal complexes offer unique potential as catalysts, sensors, and surface-modified electrodes.[1,2] In the case of polypyrrole, incorporation of metal complexes has been achieved by using metal-containing counterions[3−7] or by chemical attachment to the polymer backbone.[1,8−14] The second approach has advantages for many applications in that the metal complex is not lost from the matrix on repeated oxidation/reduction cycles of the polymer. Direct covalent attachment of metal ions or complexes to polypyrrole is complicated by the necessity of generating reactive sites on the polymer and then transporting the metal center to them. A far more common strategy is to functionalize the pyrrole monomer at either the nitrogen or the 3-position, followed by chemical or electrochemical polymerization. Despite the fact that electronic and steric effects can interfere with the polymerization reaction and that substituted polypyrroles display reduced conductivity,[15] a number of useful catalysts and sensors have been synthesized.[1,16−21]

Recently, reports have begun to appear on systems in which metal centers are electronically coupled to the conjugated polymer backbone rather than attached to the polymer by an insulating alkyl chain.[16,22−27] Early

(1) (a) Deronzier, A.; Moutet, J.-C. *Acc. Chem. Res.* **1989**, *22*, 2, 249. (b) Deronzier, A.; Moutet, J.-C. *Coord. Chem. Rev.* **1996**, *147*, 339.
(2) Curran, D.; Grimshaw, J.; Perea, S. D. *Chem. Soc. Rev.* **1991**, *20*, 391.
(3) (a) Saunders: B. R.; Fleming, R. J.; Murray, K. S. *Chem. Mater.* **1995**, *7*, 1082. (b) Saunders: B. R.; Murray, K. S.; Fleming, R. J.; McCulloch, D. G.; Brown, L. J.; Cashion, J. D. *Chem. Mater.* **1994**, *6*, 697. (c) Saunders: B. R.; Murray, K. S.; Fleming, R. J.; Korbatieh, Y. *Chem. Mater.* **1993**, *5*, 809.
(4) Mao, H.; Pickup, P. G. *J. Phys. Chem.* **1992**, *96*, 5604.
(5) Seeliger, W.; Hamnett, A. *Electrochim. Acta* **1992**, *4*, 763.
(6) Girard, F.; Ye, S.; Laperriere, G.; Belanger, D. *J. Electroanal. Chem.* **1992**, *334*, 35.
(7) Kaye, B.; Underhill, A. E. *Synth. Met.* **1989**, *28*, C97.
(8) (a) Eaves, J. G.; Munro, H. S.; Parker, D. *J. Chem. Soc. Chem. Commun.* **1985**, 684. (b) Eaves, J. G.; Munro, H. S.; Parker, D. *Inorg. Chem.* **1987**, *26*, 644.
(9) (a) Bidan, G.; Divisia-Blohorn, B.; Kern, J.-M.; Sauvage, J.-P. *J. Chem. Soc., Chem. Commun.* **1988**, 723. (b) Collin, J. P.; Jouaiti, A.; Sauvage, J.-P. *J. Electroanal. Chem.* **1990**, *86*, 275. (c) Bidan, G.; Divisia-Blohorn, B.; Mieczyslaw, L.; Kern, J.-M.; Sauvage, J.-P. *J. Am. Chem. Soc.* **1992**, *114*, 5986.
(10) Inagaki, T.; Hunter, M.; Yang, X. Q.; Skotheim, T. A.; Okamoto, Y. *J. Chem. Soc., Chem. Commun.* **1988**, 126.
(11) (a) Ochmanska, J.; Pickup, P. G. *Can. J. Chem.* **1991**, *69*, 653. (b) Ochmanska, J.; Pickup, P. G. *J. Electroanal. Chem.* **1991**, *287*, 197.
(12) Yamamoto, T.; Yoneda, Y.; Maruyama, T. *J. Chem. Soc., Chem. Commun.* **1992**, 1652.
(13) (a) Deronzier, A.; Moutet, J.-C.; Zsoldos, D. *J. Phys. Chem.* **1994**, *98*, 3086. (b) Dunand-Sauthier, M.-N. C.; Deronzier, A.; Moutet, J.-C.; Tingry, S. *J. Chem. Soc., Dalton Trans.* **1996**, 2503.
(14) Bedioui, F.; Deunyck, J.; Bied-Charreton, C. *Acc. Chem. Res.* **1995**, *28*, 30.
(15) Diaz, A. F. *Chem. Scr.* **1981**, *17*, 145.
(16) Rau, J.-R.; Lee, J.-C.; Chen, S.-C. *Synth. Met.* **1996**, *79*, 69.
(17) Creager, S. E.; Raybuck, S. A.; Murray, R. W. *J. Am. Chem. Soc.* **1986**, *108*, 4225.
(18) Franco, C. V.; Prates, P. B.; de Moraes, V. N.; Paula, M. M. S. *Synth. Met.* **1997**, *90*, 81.
(19) Sauvage, J.-P.; Collin, J.-P.; Chambron, J.-C.; Guillerez, S.; Coudret, C.; Balzini, V.; Barigelletti, F.; De Cola, L.; Flamigni, L. *Chem. Rev.* **1994**, *94*, 993.
(20) Zhao, W.; Marfurt, J.; Walder, L. *Helv. Chem. Acta* **1994**, *77*, 351.
(21) Foulds, N. C.; Lowe, C. R. *Anal. Chem.* **1988**, *60*, 2473.
(22) Cameron, C. G.; Pickup, P. G. *Chem. Commun.* **1997**, 303.
(23) (a) Hirao, T.; Higuchi, M.; Hatano, B.; Ikeda, I. *Tetrahedron Lett.* **1995**, *36*, 5925. (b) Higuchi, M.; Ikeda, I.; Hirao, T. *J. Org. Chem.* **1997**, *62*, 1072.
(24) Wolf, M. O.; Wrighton, M. S. *Chem. Mater.* **1994**, *6*, 1526.
(25) (a) Reddinger, J. L.; Reynolds, J. R. *Macromolecules* **1997**, *30*, 673. (b) Reddinger, J. L.; Reynolds, J. R. *Synth. Met.* **1997**, *84*, 225.
(26) (a) Zhu, S. S.; Swager, T. M. *J. Am. Chem. Soc.* **1997**, *119*, 12568. (b) Zhu, S. S.; Swager, T. M. *Adv. Mater.* **1996**, *8*, 8713.

10.1021/cm980332r CCC: $15.00
Published on Web 10/15/1998

evidence suggests that the conducting polymer enhances communication between the metal centers, improving redox conductivity and leading to novel physical and chemical properties. The application of this strategy to derivatized polypyrroles, however, has received little attention. Several metal−*N*-pyrrolyl complexes have been reported in the literature and might serve as monomers for very interesting polymeric materials.[28−34] Many of these are of very limited air, moisture, or thermal stability, while others have obviously unsuitable geometries. To form a highly conducting material, the complex must not have excessive steric interactions that would prevent coupling. In addition, the resulting polymer must have a conformational energy minimum in which the polypyrrole backbone is nearly planar.[15] $Fe(\eta^5\text{-}C_5H_5)(\eta^1\text{-}NC_4H_4)(CO)_2$ (Fp-pyr, **1**) meets these

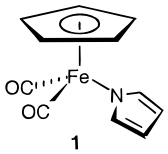

1

requirements.[35,36] Recent X-ray crystallography and computer modeling studies in our laboratories showed that **1** had suitable geometric and electronic features for oxidative polymerization.[37] Films with electrical conductivities as high as 0.25 S cm^{-1} have been prepared and characterized.

Here, we report the synthesis and structures of four new transition metal−pyrrolyl complexes. Each is sterically and electronically capable of oxidative polymerization through the pyrrolyl ligand, and each forms semiconducting polymers under the appropriate reaction conditions.

Experimental Section

General Methods. All experiments were carried out under nitrogen using Schlenk techniques or a drybox. The ^1H and ^{13}C NMR were recorded on a Varian VXR 300S spectrometer. Samples were prepared using appropriate deuterated solvents. Elemental analysis was performed by Atlantic Microlabs (Norcross, GA) or on a Perkin-Elmer Series II CHNS/O 2400 analyzer. Thermal analysis was performed on a Perkin-Elmer Series 7 thermogravimetric analyzer containing the TGA7 software package. Conductivities were measured using the four-point probe method.

6-Phenyl-2,2′-bipyridine was prepared by the method of Constable et al.[38] Methylene chloride, hexane, and toluene were freshly distilled under argon from CaH_2. Tetrahydrofuran (THF) and diethyl ether were distilled from sodium/benzophenone. Pyrrole was purchased from Aldrich and distilled before each use. Butyllithium (15% in heptane) was purchased from Eastman Kodak Co. Palladium(II) chloride, anhydrous nickel(II) chloride, potassium tetrachloropalladate, and all other chemicals were purchased from Aldrich and used without further purification.

Molecular Modeling. Density functional theory (DFT) calculations on the monomers were performed on a Silicon Graphics O_2 computer using the Spartan (version 5.0) modeling package.[39] The starting geometries for the radical cations of **3** and **5** were taken from single-crystal X-ray diffraction data of the corresponding neutrals, while those of the cations of **2** and **4** were derived from the crystal structure of neutral **3**. Bond distances and angles for these complexes were maintained as in **3** wherever possible. Each of the resulting structures were then optimized using the perturbative Becke−Perdew (pBP) nonlocal density model with a double numerical (DN) basis set.[40] The spin distributions of the radical cations of **2**−**5** were then calculated using the pBP/DN model.

Energy maps for the rotation of dimers were created using the CAChe (version 3.9) modeling package.[41] Initial structures **6**−**9** were built by coupling monomers of **2**−**5**. Each structure was minimized using the MM2 force field[42] with the CAChe extended parameter set.[43] The dihedral angle defined by the pyrrole nitrogen atoms and the pyrrole−pyrrole linkage was rotated in 10° increments from 0° (pyrroles parallel) to 180° (pyrroles antiparallel). The geometry was optimized at each step.

The spin densities of the lowest energy geometries (as predicted by MM2) of dimers **6**−**9** were calculated by the pBP/DN model. In the case of **8**, the slightly higher energy antiparallel orientation was examined rather than the slightly lower energy eclipsed orientation. No attempt to refine the geometries by density function methods was made due to the large number of basis functions. Tables of the calculated geometries of **2**, **4**, and **6**−**9** as well as the calculated condensed Mulliken population analysis for **2**−**9** can be found in the Supporting Information.

X-ray Crystallographic Analysis. Intensity data for both compounds were measured at 22 ± 1 °C by using $\omega/2\theta$ scans ($2\theta_{max}$ = 50° for **3**, 55° for **5**) with graphite-monochromated Mo Kα radiation (λ = 0.710 73 Å); measurements for **3** were made on a Nicolet R3mV diffractometer, and those for **5** were made on a rotating anode-based (18 kW) Rigaku AFC7R diffractometer. Periodic measurement of three intensity standards indicated no need for a decay correction for **3** but showed 47% decline over the course of the experiment for **5**; a linear correction was applied to the data to account for crystal decomposition in **5**. Absorption corrections based on azimuthal scans (ψ-scans) of several moderately intense reflections resulted in normalized transmission factors of 0.89−1.00 for **3** and 0.93−1.00 for **5**; Lorentz and polarization corrections were also applied to the data for both compounds. The structures were solved by using direct methods and refined by using full-matrix least-squares techniques. All nonhydrogen atoms were refined anisotropically. Hydrogen atoms were placed in optimized positions (d(C−H) = 0.96 Å) and were allowed to ride on the atom to which they were bonded; isotropic group thermal parameters were refined for all of the hydrogen atoms in each compound (U_{iso}(H): 0.076(2) $Å^2$ for **3**;

(27) Peng, Z.; Yu, L. *J. Am. Chem. Soc.* **1996**, *118*, 3777.
(28) Pannell, K. H.; Kalsotra, B. L.; Parkanyi, C. *J. Heterocycl. Chem.* **1978**, *15*, 1057.
(29) (a) Reagen, W. K.; Radonovich, L. J. *J. Am. Chem. Soc.* **1987**, *109*, 2193. (b) Reagen, W. K.; Radonovich, L. J. *J. Am. Chem. Soc.* **1989**, *111*, 3881.
(30) Edema, J. H.; Gambarotta, S.; Meetsma, A.; Bolhuis, F.; Spek, A. L.; Smeets, W. J. J. *Inorg. Chem.* **1990**, *29*, 2147.
(31) (a) Vann Bynum, R.; Hunter, W. E.; Rogers, R. D.; Atwood, J. L. *Inorg. Chem.* **1980**, *19*, 2368. (b) Vann Bynum, R.; Zhang, H.-M.; Hunter, W. E.; Atwood, J. L. *Can. J. Chem.* **1986**, *64*, 1304.
(32) Yu, Y.; Wang, S.; Ma, H.; Ye, Z. *Tetrahedron* **1992**, *11*, 265.
(33) Pommier, J. C.; Lucas, D. *J. Organomet. Chem.* **1973**, *57*, 139.
(34) Johnson, T. J.; Arif, A. M.; Gladysz, J. A. *Organometallics* **1993**, *12*, 4728.
(35) Pauson, P. L.; Quazi, A. R. *J. Organomet. Chem.* **1967**, *7*, 321.
(36) Zakrzewski, J.; Giannotti, C. *J. Organomet. Chem.* **1990**, *388*, 175.
(37) (a) Martin, K.; Dotson, M.; Litterer, M.; Hanks, T. W.; Veas, C. *Synth. Met.* **1996**, *78*, 161. (b) Powell, M.; Bailey, R. D.; Eagle, C. T.; Schimek, G. L.; Hanks, T. W.; Pennington, W. T. *Acta Crystallogr.* **1997**, *C53*, 1614. (c) Martin, K. F.; Hanks, T. W. *Organometallics* **1997**, *16*, 4857.
(38) Constable, E. C.; Henney, R. P. G.; Leese, T. A. *J. Chem. Soc., Dalton Trans.* **1990**, 443.
(39) Wavefunction, Inc., 18401 Von Karman, Suite 370, Irvine, CA 92715.
(40) (a) Becke, A. D. *Phys. Rev. A* **1988**, *38*, 3089. (b) Perdew, J. P. *Phys. Rev. B* **1986**, *33*, 8822.
(41) CAChe Scientific/Oxford Molecular, P.O. Box 500, Mail Station 13-400, Beaverton, OR 97077.
(42) Burkert, U.; Allinger, N. L. *Molecular Mechanics*; ACS Monograph 177; American Chemical Society: Washington, DC, 1982.
(43) Purvis, G. D., III. *Comput. Aided Mol. Des.* **1991**, *5*, 65.

Table 1. Summary of Crystallographic Data for Compounds 3 and 5

	compd **3**	compd **5**
formula	$C_{18}H_{16}N_4Pd$	$C_{10}H_{22}NP_2ClNi$
M_r	394.75	312.39
cryst system	monoclinic	monoclinic
space group	$P2_1/c$ (No. 14)	$P2_1/c$ (No. 14)
a (Å)	12.499(2)	13.714(4)
b (Å)	15.537(2)	10.340(6)
c (Å)	17.009(2)	11.381(6)
β (deg)	97.38(1)	109.27(3)
V (Å^3)	3275.6(7)	1523(1)
Z	8	4
D_c (g cm^{-3})	1.60	1.36
μ (mm^{-1})	1.14	1.63
transm coeff	0.89/1.00	0.93/1.00
$R(F_o)^a$	0.0244	0.0435
$R_w(F_o)^b$	0.0286	0.0540
no. of obsd data ($I > 2\sigma(I)$)	4217	2071

^{a} $R = \sum||F_o| - |F_c||/\sum|F_o|$. ^{b} $R_w = [\sum w(|F_o| - |F_c|)^2/\sum w(F_o)^2]^{1/2}$.

0.104(4) Å^2 for **5**). Structure solution, refinement, and the calculation of derived results were performed with the SHELX-TL-Plus[44] package of computer programs. Neutral atom scattering factors were those of Cromer and Waber,[45] and the real and imaginary anomalous dispersion corrections were those of Cromer.[46] Relevant crystallographic data are given in Table 1.

Synthesis of Bis(pyridyl)bis(pyrrolyl)palladium(II) ($Pd(py)_2(pyr)_2$, 2). Palladium(II) chloride (5.05 g, 28.5 mmol) was combined with 100 mL of pyridine and a stirbar in an airless flask. The flask was attached to a condenser and heated under nitrogen. The mixture was heated at reflux for 5 h and then cooled. Bis(pyridyl)palladium(II) chloride ($PdCl_2(py)_2$) was collected as yellow solid by filtration.

In an airless flask, pyrrole (10.0 mL,144 mmol) was added to distilled THF (30.0 mL) with stirring. The flask was purged with N_2, and *n*-butyllithium (13.0 mL, 138 mmol) was added dropwise over a period of 15 min to give a solution of lithium pyrrole. $PdCl_2(py)_2$ (1.52 g, 4.53 mmol) was then added to the green solution and stirred for an additional 2 h. The reaction mixture was filtered using an airless filter, and the solvent was removed in vacuo. The solid product, **2**, was washed with hexane and then toluene and air-dried. Yield: 1.41 g (3.54 mmol, 78.1%). ^{1}H NMR ($CDCl_3$, δ): 7.92 d (4 H, α-NC_5H_5); 7.34 t (2 H, γ-NC_5H_5); 7.12 t (4 H, β-NC_5H_5); 6.44 t (4 H, α-NC_4H_4); 6.14 t (4 H, β-NC_4H_4). ^{13}C NMR ($CDCl_3$, δ): 152.5 (α-NC_4H_4); 138.5 (γ-NC_5H_5); 126.5 (α-NC_5H_5); 124.8 (β-NC_5H_5); 127.3 (β-C_4H_4). Anal. Calcd for $C_{18}H_{18}N_4Pd$: C, 54.49; H, 4.57; N, 14.12. Found: C, 53.66; H, 4.23; N, 13.64.

Synthesis of (2,2′-Bipyridyl)bis(pyrrolyl)palladium(II) ($Pd(bipy)(pyr)_2$, 3). Palladium(II) chloride (1.03 g, 5.81 mmol) was added to a flask containing 20 mL of 95% ethanol. A solution of 2,2′-dipyridyl (1.12 g, 7.10 mmol) in 25 mL of 95% ethanol was added dropwise to the vigorously stirring palladium dichloride at room temperature. Stirring continued for 18 h. (2,2′-Bipyridyl)palladium(II) chloride ($Pd(bipy)Cl_2$) was isolated as a light yellow solid after washing with acetone.

A solution of lithium pyrrole in THF (30.0 mL) was prepared as above. After 20 min of stirring, $Pd(bipy)Cl_2$ (1.72 g, 5.16 mmol) was added to the Li−pyrrole solution and stirred for 2 h. The solvent was then removed in vacuo and the solid washed with hexane and allowed to dry. Yield: 1.51 g (3.83 mmol, 65.8%). ^{1}H NMR ($CDCl_3$, δ): 7.94−8.03 q (4 H); 7.59 d (2 H); 7.43 t (2 H); 6.82 t (4 H, α-NC_4H_4); 6.23 t (4 H, β-NC_4H_4). Anal. Calcd for $C_{18}H_{16}N_4Pd$: C, 54.77; H, 4.09; N, 14.29. Found: C, 53.98; H, 4.13; N, 13.89.

(44) Sheldrick, G. M. *SHELXTL-Plus (Version 4.2), Crystallographic Computing System*; Nicolet Instruments Division: Madison, WI, 1986.

(45) Cromer, D. T.; Waber, J. T. *International Tables for X-ray Crystallography*; The Kynoch Press: Birmingham England, 1974; Vol. IV, Table 2.2B.

(46) Cromer, D. T. *International Tables for X-ray Crystallography*; The Kynoch Press: Birmingham England, 1974; Vol. IV, Table 2.3.1.

Synthesis of (6-Phenyl-2,2′-bipyridyl)palladium(II) Chloride. 6-Phenyl-2,2′-bipyridine[38] (0.0240 g, 0.103 mmol) dissolved in 2.5 mL of acetonitrile was added to a solution of potassium tetrachloropalladate (0.0330 g, 0.114 mmol) and 2.50 mL of water. The solution was then heated at reflux for 24 h. Upon cooling, yellow crystals precipitated and were collected by filtration, washed with water, and allowed to dry. ^{1}H NMR (CD_3SOCD_3, δ): 8.66 d (1 H, H$^{6'}$); 8.53 d (1 H, H^3); 8.20 m (3 H, H,[4] H$^{4'}$, H$^{3'}$); 8.04 d (1 H, H^5); 7.80 d (1H, H$^{5'}$); 7.66 d (1 H, H$^{3''}$); 7.43 d (1 H, H$^{6''}$); 7.09 m (2 H, H$^{4''}$, H$^{5''}$). NMR results were consistent with literature values.[38]

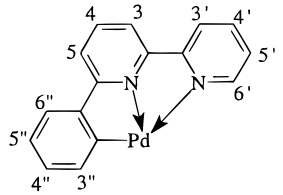

Synthesis of (6-Phenyl-2,2′-bipyridine)(pyrrolyl)palladium(II) (Pd(bipyPh)(pyr), 4). A solution of lithium pyrrole in THF (10 mL) was prepared as above. Pd(phbipy)Cl (1.49 g, 3.99 mmol) was added to the green solution and stirred for an additional 2 h. The reaction mixture was then filtered under nitrogen and the solvent removed in vacuo. Pd(bipyPh)(pyr) was purified by dissolving product in methylene chloride and precipitating it by adding solution dropwise into excess hexane. The yellow product was then collected by filtration. Yield: 0.846 g (2.09 mmol, 52.4%). ^{1}H NMR ($CDCl_3$, δ): 8.39 d (1 H, H$^{6'}$); 7.86−7.98 m (3 H, H^3, H$^{3'}$, H$^{4'}$); 7.56−7.66 m (2 H, H,[4] H^5); 7.40−7.49 m (2 H, H$^{3''}$, H$^{5'}$); 7.19 d (1 H, H$^{6''}$); 7.09−7.14 m (2 H, H$^{4''}$, H$^{5''}$); 7.04 d (2 H, α-NC_4H_4); 6.41 t (2 H, β-NC_4H_4). Anal. Calcd for $C_{20}H_{15}N_3Pd$: C, 59.49; H, 3.74; N, 10.41. Found: C, 59.03; H, 3.57; N, 9.89.

Synthesis of Bis(trimethylphosphino)nickel(II) Chloride. Anhydrous $NiCl_2$ (8.40 g, 64.8 mmol) was added to an airless flask, capped with a septum and purged with dry nitrogen. Absolute ethanol (104 mL, deoxygenated) was added to the flask and the mixture stirred, with gentle heating, for 20 min to give a light orange solution. Trimethylphosphine (1 M in THF, 59.0 mL, 59.0 mmol) was then slowly added via syringe. Stirring and gentle heating was continued for an additional 45 min, with the solution turning purple. The solution was allowed to cool to room temperature and then cooled further to −20 °C for 3 h. The resulting suspension was filtered under nitrogen to give brick red crystals of Ni(PMe_3)$_2Cl_2$ (5.35 g, 19.0 mmol, 64.3%). ^{1}H NMR (C_6D_6, δ): 0.94 s ($P(CH_3)_3$). ^{13}C NMR (C_6D_6, δ): 13.45 ($P(CH_3)_3$).

Synthesis of Bis(trimethylphosphino)(pyrrolyl)nickel(II) Chloride ($Ni(PMe_3)_2(pyr)Cl$, 5). Ni(PMe_3)$_2Cl_2$ (1.50 g, 5.35 mmol) was placed in an airless flask, capped with a septum and purged with nitrogen. Dry, deoxygenated ethyl ether (82 mL) was added, and the solution was cooled to −30 °C. Lithium pyrrole (prepared as above, 13.6 mL, 5.44 mmol) was added via syringe, and the resulting solution was stirred at −30 °C for 25 min. The flask was slowly warmed to room temperature and stirred for 4.5 h. The solvent was removed, and the residual solid was extracted with dry ether (2 × 23 mL). The extract was cooled to −20 °C overnight, and dark maroon, air-sensitive crystals of bis(trimethylphosphino)(pyrrolyl)nickel(II) chloride were isolated. Yield: 0.818 g (2.16 mmol 49.7%). ^{1}H NMR ($CDCl_3$, δ): 6.46 d (2 H, α-NC_4H_4); 6.11 d (2 H, β-NC_4H_4); 1.18 br s (18 H, $P(CH_3)_3$). ^{13}C NMR ($CDCl_3$, δ): 154.6 (α-NC_4H_4); 125.9 (β-NC_4H_4); 12.8 ($P(CH_3)_3$). Anal. Calcd for $C_{10}H_{22}ClNNiP_2$: C, 38.45; H, 7.10; N, 4.48. Found: C, 37.72; H, 6.82; N, 3.99.

General Procedure for Polymerization Using Phosphomolybdic Acid. Phosphomolybdic Acid, PMA (0.90 g, 0.49 mmol), was dissolved in 5 mL of THF to make a bright yellow solution. The selected monomer (0.1−0.4 g) was also dissolved in 5 mL of THF (often requiring extended stirring) and was filtered to remove any undissolved monomer. The two solutions were then purged with nitrogen and placed in a

moisture-free drybox. The two solutions were mixed in a glass dish. The mixtures began to change colors varying in time from immediately to several hours. The solvent was allowed to evaporate yielding a black film.

General Procedure for Polymerization Using $(Bu_4N)_2S_2O_8$ and Dodecyclbenzenesulfonic Acid (DBSA). The selected monomer (11.0 mmol) and DBSA (1.71 g, 5.24 mmol) were dissolved in 25.0 mL of benzyl alcohol and cooled to approximately 10 °C. A solution of tetrabutylammonium persulfate (1.50 g, 2.20 mmol) in 15.0 mL of benzyl alcohol was added dropwise. The reaction mixture was stirred, kept below 10 °C for 2 h, and then allowed to warm slowly to room temperature, with continued stirring, for 20 h. The reaction was terminated by pouring methanol into the reaction vessel and stirring.

Results and Discussion

Synthesis of Monomers. The synthesis of compounds **2**−**5** was achieved by first treating the appropriate metal halide with donor ligands (eqs 1 and 2). This

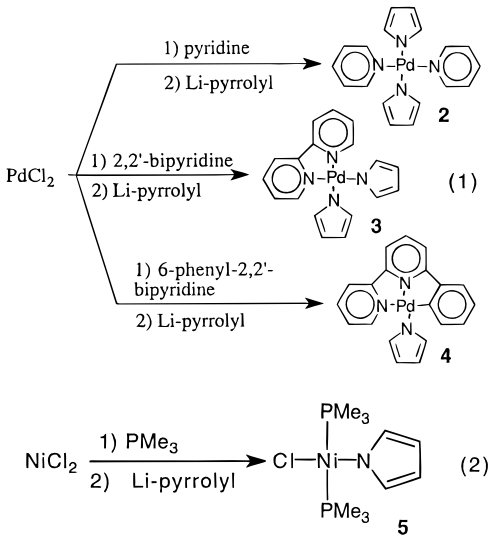

breaks up the metal chloride polymers to give moderately soluble, square planar molecular complexes. The tridentate ligand 6-phenyl-2,2′-bipyridine (bipyPh), used in the preparation of **4**, is not commercially available and was synthesized by a previously reported procedure.[38] In addition to coordinating to the bipyridyl moiety of the ligand, the palladium inserts itself into an aryl C−H bond of the phenyl ring, followed by reductive elimination of HCl to give Pd(bipyPh)Cl.

Reaction of the lithium salt of pyrrole with the metal halides results in rapid exchange of the pyrrolyl anion with the halogen. The previously unreported compounds **2**−**5** were characterized spectroscopically and, in the cases of **3** and **5**, by single-crystal X-ray diffraction. Compound **2** is assumed to have the pyrrolyl ligands trans to one another, but this has not been definitively established. The palladium complexes are moderately air- and moisture-stable in the solid state but decompose slowly in solution. Nickel compound **5** is air-sensitive and requires Schlenk techniques for manipulation. Decomposition is accompanied by a dramatic color change (solutions went from deep purple to colorless) as well as an obvious odor of PMe_3.

X-ray Structures of 3 and 5. $Pd(bipy)(pyr)_2$, **3** (Figure 1), crystallizes in the monoclinic space group $P2_1/c$ (No. 14), with two molecules per asymmetric unit.

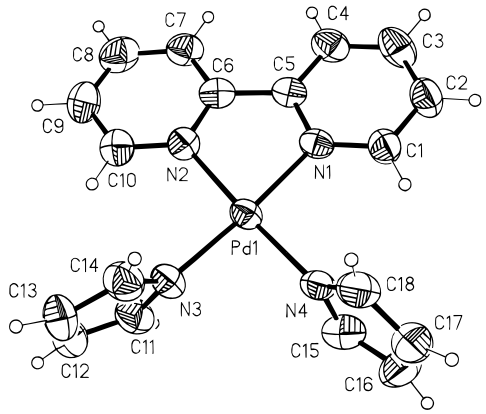

Figure 1. Thermal ellipsoid plot (50% probability) of **3** (molecule one).

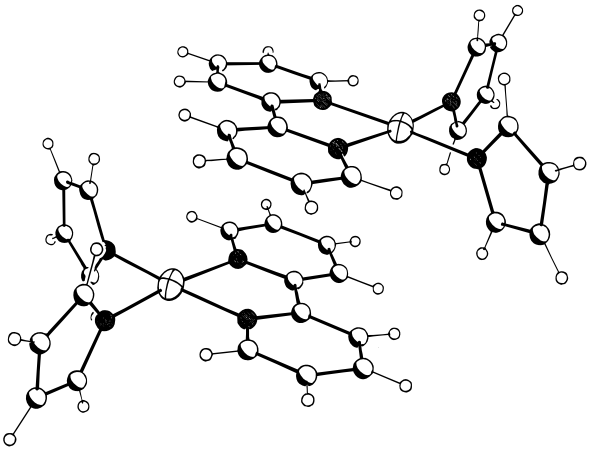

Figure 2. Inversion-related dimer of **3** (molecule one pair).

The bipy ligands for both molecules are planar (within 0.022−0.029 Å), as are the pyrrole rings (within 0.001−0.003 Å). The conformation of molecule two is slightly flatter than molecule one, as the dihedral angles of the pyrrole rings with the Pd-coordination plane (PdN4) are smaller (73.5 and 82.3° for molecule two vs 83.9 and 86.3° for molecule one). Both molecules one and two in the asymmetric unit associate with an inversion related partner to form dimers whose bpy ligands are parallel and overlapped (Figure 2). The interplanar distances for these dimers are 3.53(3) Å for molecule one and 3.48(3) Å for molecule two. The unit cell contains eight molecules, each occupying a general position within the cell.

$Ni(PMe_3)_2(pyr)Cl$, **5**, crystallizes in the monoclinic space group $P2_1/c$ (No. 14), with one molecule per asymmetric unit. The pyrrole ring is planar to within 0.0007 Å and makes a dihedral angle of 90.6° with the coordination plane of the complex which is planar to within 0.0109 Å (Figure 3). The trimethylphosphine ligands adopt a staggered orientation with respect to one another. The unit cell contains four molecules, each occupying a general position within the cell.

Molecular Modeling. The commonly accepted mechanism for the oxidative polymerization of pyrroles involves the initial generation of radical cations, which then undergo radical−radical coupling, followed by elimination of H^+ to regenerate the aromatic system.[47] The resulting dimers are even more susceptible to

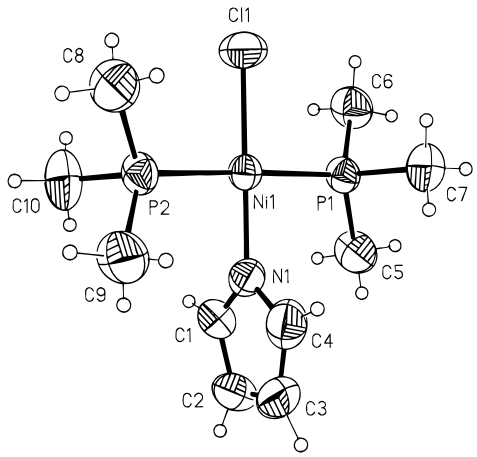

Figure 3. Thermal ellipsoid plot (50% probability) of **5**.

oxidation than the starting pyrrole and quickly repeat the process. Key to this reaction is the spin density distribution in the radical cation. Coupling at the α positions leads to a conjugated polymer, while coupling at the β position gives defects that limit the ultimate conductivity of the system. In our polymers, there are other sites on the monomer at which the unpaired electron might possibly be localized, including the metal or other ligands. An understanding of the electronic structure of new monomers is an important element of the molecular engineering of high performance electroactive materials.

Early attempts to model the spin density of pyrrole and small oligomers made use of semiempirical methods, most notably the INDO treatment.[48] We also have made use of this treatment in our work with the pyrrolyl iron monomer **1**,[37] taking advantage of parameters developed by Zerner to treat the metal.[49] These parameters, however, were optimized to reproduce electronic spectra, and the method was found to be inadequate for predicting the geometries for compounds **2**−**5**. More recently, *ab initio*[50,51] and density functional theory (DFT)[51,52] calculations have been used to assist in the design of new conducting polymers. The latter approach is rapidly gaining in popularity, because the time requirements for the calculations scale less rapidly with increasing numbers of basis functions, without sacrificing accuracy. DFT methods have also been reported to give results superior to ab initio methods in systems containing metals.[53]

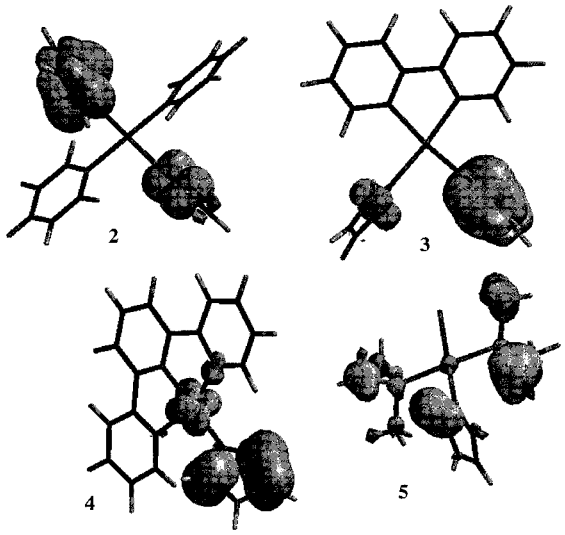

Figure 4. DFT spin density distributions of the radical cations of **2**−**5**.

Table 2. DFT Calculated Condensed Mulliken Spin Densities (×10⁴) of Compounds 2−5

	2	3	4	5
pyrrole 1, α	160	60	302	22
pyrrole 1, β	31	16	108	8
pyrrole 2, α	317	400	N/A	N/A
pyrrole 2, β	67	77	N/A	N/A
α/β ratio[a]	4.9	4.9	2.8	2.8
py/other ratio[b]	>100	>100	3.2	0.15

[a] Ratio of the average spin density at all α positions vs those at all β positions. [b] Ratio of the sum of the spin density at all pyrrole atoms vs the sum of the spin density at all other atoms.

Geometry optimization of the complexes discussed here presents a challenge at the DFT level. To keep computational time to a feasible level, full optimizations were performed only on the cations of **2** and **4**, since single-crystal X-ray data were available for **3** and **5**. In each case, a double numerical basis set (DN) was used but without polarization functions. The cations of **3** and **5** were assumed to adopt the same geometry as observed in the crystal structure of the neutral complex.

The calculated unpaired-electron spin densities for the radical cations of **2**−**5** are shown in Figure 4, while Table 2 quantifies the essential details of the calculations. The dipyrrolyl complexes $Pd(py)_2(pyr)_2$, **2**, and $Pd(bipy)(pyr)_2$, **3**, give results that are very similar to calculated (DFT) and experimental (ESR) results obtained for the radical cation of free pyrrole.[52] In each case, essentially all of the spin density lies on the pyrrolyl ligands, with the spin population being about 5 times higher at the α positions than at the β. As expected for systems in which the HOMO has π symmetry, the s-orbital contribution to the overall spin population is negligible. No symmetry was imposed on the calculations, so there are differences in the spin magnitude between the two pyrrolyl ligands. Small changes in the orientation of the two rings change these relative magnitudes but do not lead to an increase in spin density elsewhere in the molecules. Conversely, compound **4**, possessing the tridentate 6-phenyl-2,2′-bipyridine ligand, does show unpaired-electron density at both the metal and at the bipyPh ligand in addition to the pyrrolyl ligand. While approximately 75% of the total spin is on the pyrrolyl ligand at the calculated

(47) Genies, E. M.; Bidan, G.; Diaz, A. F. *J. Electroanal. Chem.* **1983**, *149*, 101.
(48) (a) Waltman, R. J.; Bargon, J. *Tetrahedron* **1984**, *40*, 3963. (b) Waltman, R. J.; Bargon, J. *Can. J. Chem.* **1986**, *64*, 76. (c) Karelson, M. Zerner, M. C. *Chem. Phys. Lett.* **1994**, *224*, 213. (d) Sanechika, K.; Yamamoto, T.; Yamamoto, A. *J. Polym. Sci., Polym. Lett. Ed.* **1982**, *20*, 365. (e) Waltman, R. J.; Diaz, A. F.; Bargon, J. *J. Phys. Chem.* **1984**, *88*, 4343. (f) Ambrose, J. F.; Nelson, R. F. *J. Electrochem. Soc.* **1968**, *115*, 1159. (g) Dessau, R. M.; Shih, S. *J. Chem. Phys.* **1970**, *53*, 3169.
(49) (a) Zerner, M. C.; Loew, G. H.; Kirchner, R. F.; Mueller-Westerhoff, U. T. *J. Am. Chem. Soc.* **1980**, *102*, 589. (b) Anderson, W. P.; Cundarai, T. R.; Drago, R. S.; Zerner, M. C. *Inorg. Chem.* **1990**, *29*, 1.
(50) Champagne, B.; Mosley, D. H.; Fripiat, J. G.; Andre, J.-M. *Phys. Rev. B* **1996**, *54*, 2381.
(51) Viruela, P. M.; Viruela, R.; Orti, E.; Bredas, J.-L. *J. Am. Chem. Soc.* **1997**, *119*, 1360.
(52) Smith, J. R.; Cox, P. A.; Campbell, S. A.; Ratcliffe, N. M. *J. Chem. Soc., Faraday Trans.* **1995**, *91*, 2331.
(53) Hehre, S. J.; Lou, L. *A Guide to Density Functional Calculations in Spartan*; Wavefunction, Inc.: Irvine, CA, 1997.

equilibrium geometry, small changes in the orientation of the pyrrolyl ligand can dramatically decrease this percentage. This effect is undoubtedly observed due to the presence of relatively high energy π-type orbitals on the tridentate bipyPh ligand. It is possible that some side reactions, including radical coupling processes, might occur on this ligand as well as on the pyrrolyl ligand. Additionally, the ratio of the spin density between the α and β positions of the pyrrolyl ligand is less than 3. This suggests that defects due to coupling at the β position might be more important in the polymerization of **4** than with either **2** or **3**.

The calculated spin density distribution in $Ni(PMe_3)_2$(pyr)Cl, **5**, is more complex than in the palladium radicals, because the frontier orbitals are broadly delocalized across the molecule. Most of the spin population is predicted to be localized on the trimethylphosphine ligands, while that located on the pyrrolyl ligand is predicted to have primarily s-symmetry. It is difficult to predict the behavior of this complex on oxidation, and indeed, we find it to be highly dependent upon conditions (below).

High conductivity in conjugated polymers requires substantial planarity of the polymer backbone in order to maximize π-overlap between adjacent rings. Polypyrrole derivatives are typically quite sensitive to steric interactions. Even the replacement of the N-bound proton with a methyl group results in a drop in conductivity of approximately 2 orders of magnitude. To examine the effect of our large transition metal functionalities on the preferred orientation of the polymer, we constructed dimers of **2**−**5** by coupling the pyrrole units via their α carbons (compounds **6**−**9**, respectively). The torsional potential of each dimer was examined by molecular mechanics,[42] using a modified MM2 force field which incorporates parameters for transition metals.[43] As previously observed in our investigations of **1**,[37] this force field maintains reasonable geometries about the metal centers, while allowing enough flexibility to emphasize the steric interactions of the organic substituents during rotation. The dihedral angle between the two rings (defined as the angle between nitrogens on adjacent pyrrolyl groups while looking down the pyrrolyl−pyrrolyl bond) was rotated in 10° increments from the fully eclipsed orientation (0°) to the anti orientation (180°) with the dimer geometry optimized at each step. The results of these calculations are summarize in Figure 5.

Unlike many derivatives of pyrrole, these square-planar transition metal complexes show an energy minimum at the anti conformation. In three of the four cases, this is a global minimum. Interestingly, the dimer of Pd(bipyPh)(pyr), **8**, has a slight preference for the orientation in which the metal centers are eclipsed. Multiple segments of eclipsed transition metal units are impossible, because the pyrrolyl backbone is not linear unless the units are staggered. However, occasional eclipsed units in polyPd(bipyPh)(pyr) or in copolymers with pyrrole might offer sites for host−guest interactions. Such sites could be exploited for sensor or catalytic devices.

Dimers **7** and **8** each have very low rotational barriers, due to their flat chelating ligands which cause little steric interaction with adjacent monomer units. Conversely, compounds **2** and **5** have the majority of their steric bulk out of the plane of the metal complex, resulting in significant rotational barriers. In all cases, we would expect that α,α-coupled extended polymer chains would be highly oriented, with substantially planar backbones.

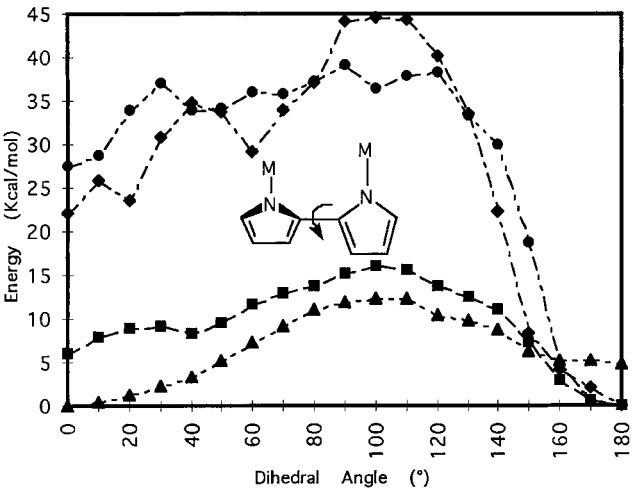

Figure 5. Relative energies of rotation in dimers **6**−**9**.

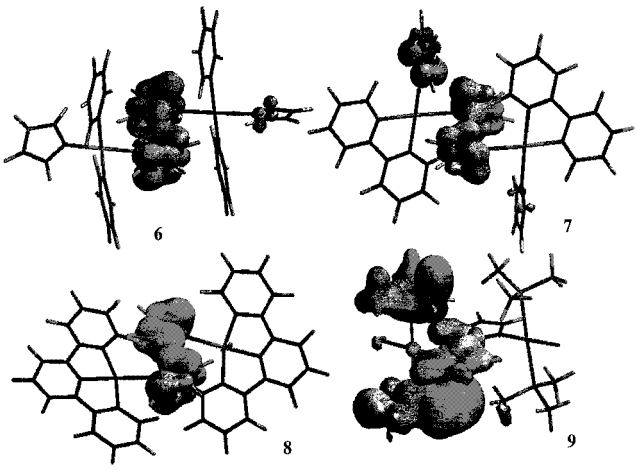

Figure 6. DFT spin density distributions of the radical cations of **6**−**9**.

We have also examined the electronic structure of radical cations that would be produced from structures **6**−**9** (Figure 6). In each case, the dihedral angle was set at 180°, while all other bond angles and distances were set as in the corresponding monomers. The radical cations of palladium complexes **6**−**8** each have spin populations which are essentially located in the π system of the conjugated pyrrolyl ligands. The results of these calculations mirror those of DFT calculations made by Cambell et al. on the bis(pyrrole) radical cation.[52] Conjugation of the pyrroles clearly localizes the high-energy orbitals which are susceptible to oxidation on the backbone π system. As with pyrrole oligomers, we expect that increased chain length will lead to an increase in spin density at the β positions and an enhanced likelihood of chain defects due to coupling at these sites.

The complex $[Pd(bipy)pyr)]_2$, **7**, also displays some spin density on the noncoupled pyrrolyl ligand. Not surprisingly, even a slight twist from planarity at the pyrrolyl−pyrrolyl linkage dramatically increases this

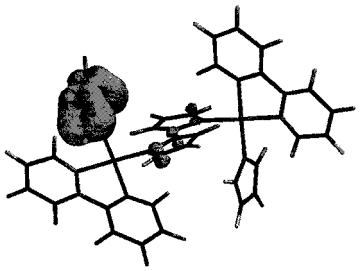

Figure 7. Spin density distribution of the radical cation of **7** when the backbone is twisted out of planarity.

effect (Figure 7). Similar results are observed with the other palladium dimers. Thus, while steric considerations favor a highly planar backbone in all of the palladium systems and this, in turn, favors coupling at the desired α carbons at the termini of the growing chains, deviations from the equilibrium geometry could lead to dramatic changes in regioselectivity. Simple entropy considerations guarantee that oligomers of **2** and **3**, each of which contain two pyrrolyl ligands per monomer, will suffer periodic twists in the growing chain. This would encourage chain growth on the other pyrrole, thus creating a defect in which the backbone passes through the metal. This situation does not arise with monopyrrolyl complexes **4** and **5**.

The radical cation of **9** shows a complex spin distribution primarily centered, as in the monomer **5**, on the phosphine ligands. Even the spin population of the pyrrolyl ligands includes contributions from both s and π symmetry elements. As with the monomer, the DFT calculations for **9** do not obviously predict polymer formation by radical coupling of pyrrolyl ligands.

Polymer Film Synthesis and Properties. In our previous work with Fp-pyr, **1**,[37] we found that electropolymerization leads to poor-quality, insulating films but that chemical oxidation could produce high-quality, semiconducting polymers. Compounds **2** and **3** also failed to polymerize electrochemically to form electroactive materials, probably due to overoxidation of the growing chains. Chemical oxidation of **2**−**5**, however, did lead to conducting materials. Three different chemical oxidation methods were examined in this study. We initially attempted the polymerization of compounds **2** and **3** by a two-phase system in which $FeCl_3$ was dissolved in water while a THF solution of a palladium complex was carefully layered on top. Very thin, jet black films grew at the interface of the two solutions. These films proved to be far too delicate to remove intact, crumbling into a completely insoluble powder. This behavior is similar to what was previously observed with the iron complex Fp-pyr (**1**).[37] Additional investigation of this route was abandoned in favor of more satisfactory methods.

We have shown that polymers of **1**, prepared by oxidation with phosphomolybdic acid, result in significantly higher quality films than those prepared by interfacial polymerization with $FeCl_3$. Phosphomolybdic acid is an exceedingly mild oxidant, and the entire reaction can be conveniently run in a drybox to prevent exposure to oxygen or moisture (this is particularly important for **5**). Compounds **2**−**5** were dissolved in dry, deoxygenated THF and added to a THF solution of phosphomolybdic acid. The palladium complexes slowly

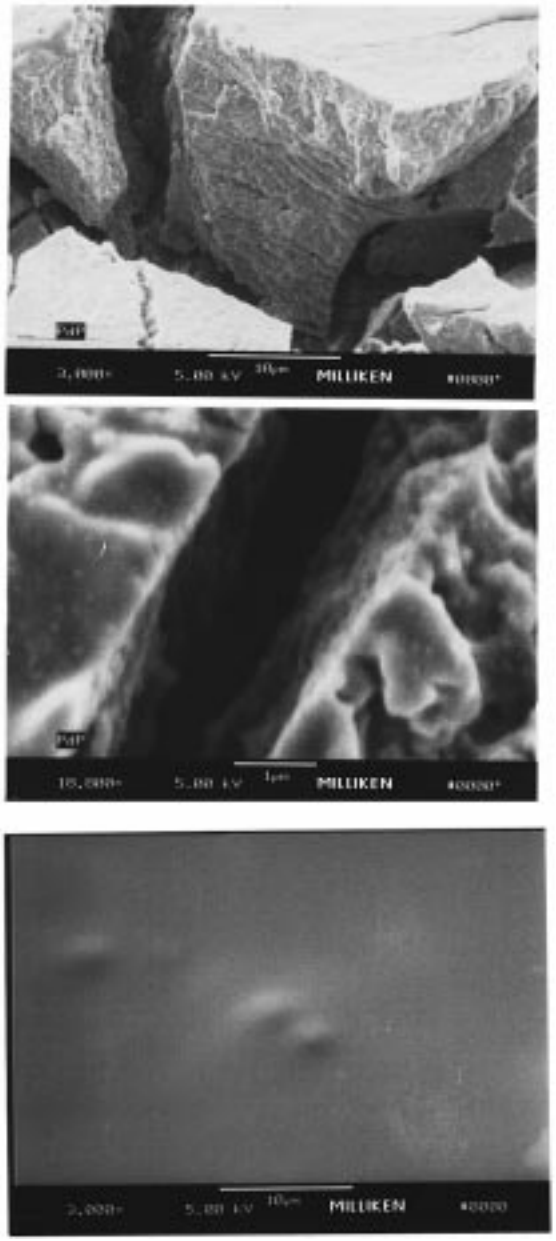

Figure 8. FEM micrographs of polymers of **2** prepared by the phosphomolybdic acid method (top, 800×; middle, 3000×) and the DBSA/TBAPS method (bottom, 3000×).

formed thick, but brittle, black films as the THF evaporated. Figure 8 shows a FEM micrograph of poly **2** at 800× and 3000× magnification. Large fractures (1−10 μm) permeate the material. At the higher magnification, the large features are shown to be composed of small granules (0.1−1 μm). This is similar to the structure of polymers of $CpFe(pyr)(CO)_2$ produced under the same conditions.

Despite its oxygen sensitivity, the nickel complex **5** was also found to polymerize with phosphomolybdic acid without apparent decomposition of the coordination complex. Unlike the palladium complexes, **5** reacted almost instantly, forming a tough, strongly adhering material that had to be broken into small pieces to be removed from the reaction vessel. The polymer showed much better air stability than the monomer, decomposing (color change, PMe_3 evolution) on the order of hours rather than minutes.

Table 3. Electrical Conductivities ($\times 10^{-4}$ S/cm) of Polymers Prepared from 2 to 5

method	2	3	4	5
phosphomolybdic acid	0.25	9.0	9.6	250
DBSA/TBAPS	0.20	7.4	11	

The third polymerization method is a modification of a procedure of Lee, Kim and Kim and was used to prepare a soluble polymer of **1** having the highest conductivities observed to date for a transition metal-derivatized polypyrrole.[37b] Dodecylbenzenesulfonic acid (DBSA) and palladium monomers **2**−**4** were dissolved in benzyl alcohol, the solution was cooled, and a benzyl alcohol solution of tetrabutylammonium persulfate (TBAPS) was added dropwise. The TBAPS serves as the oxidant, while the DBSA remains in the polymer as a counterion and surfactant. In each case, modestly soluble, electrically conducting materials were formed that could be cast into films. Their improved solubility greatly facilitated the casting of the polymers into smooth films. A FEM micrograph of a film produced from the DBSA/TBAPS polymerization of **2** (3000× magnification) is shown in Figure 8. This almost featureless film was observable only after heating in a vacuum oven (12 h, 60 °C) to remove excess DBSA. Freshly cast films were found to flow in the FEM electron beam.

The DBSA/TBAPS method was also attempted on the nickel monomer **5** without success. Under the reaction conditions, **5** immediately decomposes to give a light green, highly insoluble, insulating powder. In addition, the reaction produces a strong odor of trimethylphosphine, indicating a reaction at the metal center. No attempt was made to characterize this material.

The electrical conductivities of the polymer films prepared from **2**−**5** are shown in Table 3. The palladium-containing films can be stored in air for months without significant loss of conductivity, while the nickel-containing film begins to show degradation in a matter of hours. Surprisingly, poly(**5**) prepared by the phosphomolybdic acid route is more conductive than any of the palladium polymers. Thermal analysis of the palladium-based films reveal mass losses that are consistent with non-pyrrolyl ligand loss, followed by the slow degradation of the polymer backbone. The thermally induced loss of non-pyrrolyl ligands generally comes at slightly higher temperatures than in the corresponding monomer, reflecting the greater difficulty in diffusion from the solid matrix. The backbone stability of the palladium polymers is slightly better than that of polypyrrole when the polymers are made by the phosphomolybdic acid method. Conversely, backbone degradation of the palladium polymers prepared by the DBSA/TBAPS method is more rapid than with polypyrrole made under the same conditions. Poly(**2**) and poly(**3**) are significantly less stable, with complete backbone degradation occurring by 375 and 425 °C, respectively (vs 580 °C for polypyrrole). The backbone degradation for poly(**4**) is completed by 500 °C, and unlike poly(**2**) and poly(**3**), the distinction between ligand loss and the backbone degradation is clear.

Conclusions

Palladium complexes **2**−**4** behave much like pyrrole or Fp-pyr upon oxidation. This is because their HOMOs are essentially pyrrole π-orbitals. Polymers of these compounds display electrical conductivity which is substantially less than polypyrrole, or even polyFp-pyr, primarily because of undesired radical coupling processes. In the cases of **2** and **3**, the second pyrrolyl ligand becomes the primary reaction site when the backbone deviates from planarity. In the case of **4**, the highly conjugated bipyPh ligand competes with the pyrrole for the radical spin density. The nickel complex **5** is a different matter entirely. The compound itself is sensitive to oxidative decomposition. However, in the very mild oxidizing environment afforded by phosphomolybdic acid, side reactions are suppressed and a very tough polymer with relatively high conductivity can be produced. Additional evidence for increased selectivity in the phosphomolybdic acid route is the excellent thermal stability of all of the polymers. Conversely, the DBSA/TBAPS route produces polymers of lower backbone thermal stability than seen with polypyrrole. This is particularly evident in poly(**2**) and poly(**3**), where the presence of a second pyrrolyl ligand may lead to polymers containing very short pyrrole chains cross-linked by palladium.

Polymers and copolymers of compounds **1**−**5** show promise as materials for sensor and catalyst applications. We are currently exploring the reaction chemistry of these systems in efforts to construct useful devices.

Acknowledgment. This work was supported by a grant from the NSF (CHE 96-14966). We thank Michael Sullivan and Sally Blankton of the Milliken Research Corp. for assistance with the FEM images.

Supporting Information Available: Complete listings for **3** and **5** of crystallographic data, atomic coordinates, bonding distances and angles, and anisotropic thermal parameters, figures showing packing diagrams and a molecular plot (of **3**, molecule two), and tables of observed and calculated structure factors and Mulliken condensed spin populations of **2**−**9** (72 pages). Ordering information is given on any current masthead page.

CM980332R